NASA Technical Memorandum 104019

Computation of Wind Tunnel Wall Effects for Complex Models Using a Low-Order Panel Method

Dale L. Ashby and Scott H. Harris

February 1994

National Aeronautics and Space Administration

NASA Technical Memorandum 104019

Computation of Wind Tunnel Wall Effects for Complex Models Using a Low-Order Panel Method

Dale L. Ashby and Scott H. Harris, Ames Research Center, Moffett Field, California

February 1994

National Aeronautics and
Space Administration

Ames Research Center
Moffett Field, California 94035-1000

Nomenclature

AR	aspect ratio
b	wingspan, ft
c	local wing chord, ft
$\bar{c}$	wing mean aerodynamic chord, ft
C_L	wind-axis lift coefficient (thrust removed)
C_{L_α}	wind-axis lift-curve slope (thrust removed)
C_p	pressure coefficient
q	tunnel dynamic pressure, psf
S	wing reference area, ft^2
V_∞	tunnel free-stream velocity, knots
x	longitudinal model coordinate, positive aft, in.
y	lateral model coordinate, positive toward model right wing tip, in.
z	vertical model coordinate, positive toward model upper surface, in.
α	model angle of attack, deg
$\Delta\alpha$	change in model angle of attack due to tunnel wall effects
ΔC_L	change in model lift coefficient due to presence of tunnel walls or mounting hardware
λ	taper ratio
Λ_{LE}	leading-edge sweep angle, deg
Λ_{TE}	trailing-edge sweep angle, deg

Summary

A technique for determining wind tunnel wall effects for complex models using the low-order, three-dimensional panel method PMARC (Panel Method Ames Research Center) has been developed. Initial validation of the technique was performed using lift-coefficient data in the linear lift range from tests of a large-scale STOVL fighter model in the National Full-Scale Aerodynamics Complex (NFAC) facility. The data from these tests served as an ideal database for validating the technique because the same model was tested in two wind tunnel test sections with widely different dimensions. The lift-coefficient data obtained for the same model configuration in the two test sections were different, indicating a significant influence of the presence of the tunnel walls and mounting hardware on the lift coefficient in at least one of the two test sections. The wind tunnel wall effects were computed using PMARC and then subtracted from the measured data to yield corrected lift-coefficient versus angle-of-attack curves. The corrected lift-coefficient curves from the two wind tunnel test sections matched very well. Detailed pressure distributions computed by PMARC on the wing lower surface helped identify the source of large strut interference effects in one of the wind tunnel test sections. Extension of the technique to analysis of wind tunnel wall effects on the lift coefficient in the nonlinear lift range and on drag coefficient will require the addition of boundary-layer and separated-flow models to PMARC.

Introduction

Wind tunnel tests of scale models of aircraft or aircraft components are frequently used to obtain the force and moment coefficients that would act on the full-scale article at the same Reynolds number and Mach number. However, the presence of the wind tunnel walls and model mounting hardware can cause increments in the force and moment coefficients measured in the wind tunnel that are not present at the full-scale flight condition. The presence of the wind tunnel walls creates an increase in dynamic pressure around the model and changes the effective angle-of-attack and tail downwash angles. Model mounting hardware can create local flow-field distortions which can affect measured force and moment coefficients. Wind tunnel wall effects can be negligible if the walls are far away from the model; however, most models are scaled as large as possible for a given wind tunnel so that the test Reynolds number is as close as possible to the flight-condition Reynolds number. In order for force and moment coefficients measured in the wind tunnel to be representative of the full-scale flight condition, the wind tunnel wall effects must be removed from the data.

Most of the classical methods for computing the increments in force and moment coefficients due to the presence of wind tunnel walls represent the model with simple line vortices or point sources and doublets (ref. 1). The presence of the tunnel walls is simulated by a system of images of the singularities representing the model. These methods, however, yield a set of only global or average corrections and are not necessarily applicable for test sections having curved walls. These methods also do not address the issues of interference of mounting hardware, flow separation, or highly deflected wakes and jet flows.

Panel methods provide an alternative to the classical wall-correction techniques. In a panel method, the model surface is discretized using a set of panels. For a two-dimensional panel method, the panels are line segments that approximate the body. For a three-dimensional panel method, the panels are generally either quadrilaterals or triangles. Once the body has been discretized into a set of panels, singularities (vortices, sources, and/or doublets) of unknown strength are distributed over the panels. If the strength of the singularity is held constant along the surface of each individual panel, the panel method is low-order. High-order panel methods use singularities whose strengths vary along the surface of each panel. By applying appropriate boundary conditions to each panel, such as zero normal velocity at panel centroids, a linear system of equations for the unknown singularity strengths can be developed. Once the strengths of all the singularities are determined, the velocity vector field and the pressure field around the body can be computed.

Because a three-dimensional panel method provides a more complete representation of the model than the classical wall-correction methods, it can offer greater detail about the flow field. The potential flow field around the actual three-dimensional model geometry, both with and without the wind tunnel walls present, can be computed and the two cases compared to assess the effect of the presence of the wind tunnel walls. Curved wind tunnel walls and asymmetric test conditions can be easily simulated. Information about the interference effects of mounting hardware such as struts or sting mounts can also be obtained from the panel method solution.

In the last decade, several efforts to use panel methods to compute wind tunnel wall corrections have been reported in the literature. Ojha and Shevare (ref. 2) examined the use of a two-dimensional panel method to predict wind tunnel wall effects. Several airfoils were discretized using panels with linearly varying vortex distributions. The walls were modeled with an infinite series of images of the paneled geometry. Bowcutt (ref. 3) also used a two-dimensional panel method to compute wind tunnel wall

corrections. In this case, viscous flow phenomena, such as separated wakes, were empirically included in the modeling. Both of these studies showed encouraging results, but are of limited utility because they are restricted to two-dimensional flows. Lee (ref. 4) used a high-order, three-dimensional panel method to compute wind tunnel wall effects for a lifting wing in a wind tunnel with slotted walls. The effects of slot openness and model mounting hardware were evaluated by comparing computations for various configurations; however, no experimental validation of the computations was performed. Also, no information was given on whether it was necessary to use a high-order panel method, which is computationally more expensive than a low-order method, to accurately assess wind tunnel wall effects. Holt and Hunt (ref. 5) presented several simplified examples in two and three dimensions which illustrate the utility of panel methods for estimating wind tunnel wall effects in cases where classical techniques are inadequate. Here again, however, no experimental validation of the computations was given.

The purpose of the present study is to validate the technique of using a three-dimensional, low-order panel method for evaluating the effects of wind tunnel walls and mounting hardware on the lift coefficient of complex models. The code chosen for this study is the panel method PMARC (Panel Method Ames Research Center) (refs. 6 and 7). Since PMARC is now limited to modeling only potential flow, the computations will be restricted to the linear lift range. The validation will be accomplished by using PMARC to compute effects of the wind tunnel walls and mounting hardware on the lift coefficient of a large-scale Short Takeoff Vertical Landing (STOVL) fighter configuration that was tested in both test sections of the National Full-Scale Aerodynamics (NFAC) facility at NASA Ames Research Center (ref. 8). The computed results obtained for the two test sections will be compared to assess the validity of the technique.

Description of Model and NFAC Facility

The model used for the present study is the large-scale E-7A supersonic STOVL fighter model, shown in figure 1. The E-7A is the result of a General Dynamics design study that explored several STOVL fighter configurations (ref. 9). The model has a delta wing planform, with a NACA 630004 airfoil section and a linear twist distribution that ranges from zero degrees at the root to 6 degrees of leading-edge down twist at the wing tip. Detailed model dimensions are presented in table 1. The propulsion system of the E-7A, shown schematically in figure 2, consists of a set of chordwise ejectors located in the forward portion of the wing root and a rear nozzle, both powered by fan bypass flow, and a vectorable ventral nozzle powered by the core flow. Four different fixed-geometry ventral nozzles allow vectoring of the core flow to deflection angles of 6°, 30°, 60°, and 90°. For hover or transitional flight, fan bypass flow is directed to the ejectors and the ventral nozzle is vectored to a deflection angle of 30°, 60°, or 90° to provide vertical lift. For conventional wing-borne flight, fan flow is directed to the rear nozzle, the ejector system is closed, and the ventral nozzle is deflected at 6°. The E-7A model is powered by a Rolls-Royce Spey 801-SF split-flow turbofan capable of producing 10,450 lbf of thrust. The ventral nozzle produces 63% of the total thrust, and the ejectors or the rear nozzle produce the other 37%.

The E-7A model was tested in the NFAC facility at NASA Ames Research Center. The NFAC, shown schematically in figure 3, consists of two circuits that share a common fan drive system. The closed-return circuit has a 40- by 80-foot test section and is capable of speeds up to 300 knots. The open-return circuit has a 80- by 120-foot test section and is capable of speeds up to 100 knots. Both circuits of the NFAC allow models to be tested at near-flight Reynolds number. The size of the E-7A model relative to the test section cross-section for each tunnel can be seen in figures 4 and 5.

In both test sections, the model is supported by two fixed-length main struts at the rear of the model and by a single telescoping strut at the front of the model. The struts are enclosed in fairings to prevent aerodynamic loads on the struts themselves from being included in the total measured loads for the model. The main struts and strut fairings are made up of several sections stacked one on top of the other. A strut tip fits between the top of each main strut and the corresponding attachment point on the model. The strut tips are not enclosed in aerodynamic fairings. The top two sections of the main struts and strut fairings used in the 80- by 120-foot test section were geometrically equivalent to the main strut and strut fairing assembly used in the 40- by 80-foot test section. The strut tips used in the 80- by 120-foot test section, however, were shorter than the ones used in the 40- by 80-foot test section. This difference was necessary in order to place the model on the tunnel centerline in each test section.

Wall-Correction Computation Procedure

The tests of the E-7A model in the NFAC facility provide an ideal database for validating the technique of using a low-order panel method to evaluate wind tunnel wall effects. The same model was tested in two wind tunnel test sections of widely different dimensions (40- by

80-foot and 80- by 120-foot). The magnitude of the increment in lift coefficient due to the presence of the wind tunnel walls and mounting hardware should be considerably different for the two test sections. The wind tunnel wall effects can be computed using the low-order panel method PMARC and then subtracted from the measured data to yield corrected lift-coefficient versus angle-of-attack curves. The corrected lift-coefficient curves from the two wind tunnel test sections should match if the computed wind tunnel wall effects are accurate. This is the validation strategy pursued in the present study.

Only data from the E-7A in the conventional wing-borne flight configuration were used in this preliminary validation. Wind tunnel wall effects for the E-7A in a hover or transitional flight configuration were deemed too difficult to compute at this time due to the presence of three jets deflected at large angles to the free-stream velocity. All three jets interact strongly with the lower surface of the wing, and there are large regions of separated, turbulent flow immediately aft of each jet. In addition, there are recirculation effects as the jets impinge on the tunnel floor, particularly in the 40- by 80-foot test section. These effects could be simulated by including empirical models in the PMARC code, but this was not pursued in the current study.

Figure 6 shows the PMARC representation of the E-7A in the conventional wing-borne flight configuration without the wind tunnel present. A total of 2,336 panels were used to model the E-7A. A flat wake 20 chord lengths long was attached to the wing trailing edge. Normal velocities were specified on the engine inlet and on the ventral nozzle and rear nozzle exhausts to simulate the flow through the engine.

The PMARC representation of the E-7A in the 40- by 80-foot test section of the NFAC is shown in figure 7. The E-7A in this model is identical to the one shown in figure 6. The test section walls were simulated by a constant-area tube extending 25 chord lengths downstream of the E-7A and 2 chord lengths upstream of the E-7A. The turntable and the main-strut and nose-strut fairings are included in the PMARC representation of the 40- by 80-foot test section. The strut fairings are attached to the turntable so that when the E-7A is yawed in the PMARC model, the strut fairings will be in the proper position and orientation, allowing the computation of wall effects for cases when the E-7A is yawed. The strut tips that extend from the top of the fairings to the attachment points on the E-7A (see fig. 1) are not modeled. The number of panels needed to model the 40- by 80-foot test section was 1,899, with 750 of these used for the strut fairings. Figure 8 shows a similar PMARC representation of the E-7A in the 80- by 120-foot test section of the NFAC.

The general procedure for computing the increment in lift coefficient due to the presence of the wind tunnel walls and model support hardware is as follows. PMARC is used to compute the lift coefficient of the E-7A alone at several angles of attack in the linear lift range. Next, the lift coefficient of the E-7A model with the wind tunnel strut fairings added is computed at the same angles of attack. Finally, PMARC is used to compute the lift coefficient of the E-7A model with the strut fairings and the wind tunnel walls present, again at the same angles of attack. The three computed lift-coefficient versus angle-of-attack curves can then be compared to assess the effects of the wind tunnel walls and mounting hardware.

The lift-coefficient versus angle-of-attack curves for the E-7A alone, for the E-7A with strut fairings, and for the E-7A with strut fairings and wind tunnel walls present are all plotted as straight lines (see figs. 9 and 10). The difference between the lift coefficient for the E-7A with strut fairings and the lift coefficient for the E-7A alone at a given angle of attack represents the increment in lift coefficient due to the presence of the strut fairings as a function of angle of attack. The difference between the lift-coefficient versus angle-of-attack curves for the E-7A with strut fairings and those for the E-7A with strut fairings and wind tunnel walls is caused by the interference effect of the wind tunnel walls. In general there will be two differences between the curves: a difference in slope and a difference in zero-lift angle of attack. The change in slope can be looked at as an effective change in dynamic pressure at the model due to the presence of the walls, and the change in zero-lift angle of attack can be looked at as an effective change in model angle of attack. Since only the linear portion of the lift curve is being considered, these two quantities are sufficient to provide the transformation required to convert the lift-coefficient versus angle-of-attack curve obtained in the wind tunnel to an equivalent curve with wind tunnel wall effects removed. The methodology is summarized in the following equations:

$$\Delta C_{L_{\text{strut fairings}}} = C_{L_{\text{E-7A/strut fairings}}} - C_{L_{\text{E-7A alone}}} \quad (1)$$

$$C_{L_{\text{corrected}}} = C_{L_{\text{measured}}} * \frac{C_{L_{\alpha_{\text{E-7A/strut fairings}}}}}{C_{L_{\alpha_{\text{E-7A/strut fairings/tunnel walls}}}}} - \Delta C_{L_{\text{strut fairings}}} \quad (2)$$

$$\alpha_{corrected} = \alpha_{measured} - \Delta\alpha \quad (3)$$

$$\Delta\alpha = (\alpha)_{C_{L_{E\text{-}7A/strut\ fairings/tunnel\ walls=0}}} - (\alpha)_{C_{L_{E\text{-}7A/strut\ fairings=0}}} \quad (4)$$

Thus the corrections for slope change, zero-lift coefficient intercept change, and lift-coefficient change due to strut interference can be applied to experimental lift-coefficient data for the same configuration to remove the interference effects of the wind tunnel walls and the mounting hardware.

Results and Discussion

The PMARC data plotted in figure 9 served as the basis for obtaining the wind tunnel wall effects for the E-7A model in the conventional wing-borne flight configuration in the 40- by 80-foot test section of the NFAC. The effect of the strut fairings on the lift coefficient was evaluated using equation (1). $\Delta C_{L_{strut\ fairings}}$ showed negligible variation with angle of attack for the 40- by 80-foot test section strut fairings. The 40- by 80-foot test section strut fairings induce a uniform decrease in the lift coefficient of approximately 0.004. The presence of the 40- by 80-foot test section walls causes an increase in the lift curve slope of approximately 10% as well as a negative shift in the zero-lift angle of attack of about 0.4°. It is evident from figure 9 that the wind tunnel walls contribute the majority of the interference effects. The actual magnitudes of the corrections are summarized in table 2.

The PMARC results shown in figure 10 were used to evaluate the wind tunnel wall effects for the E-7A in the 80- by 120-foot test section of the NFAC. In this case, $\Delta C_{L_{strut\ fairings}}$ varied linearly with angle of attack, although the slope was still quite small. The intercept of the $\Delta C_{L_{strut\ fairings}}$ versus angle-of-attack curve, however, is more than four times larger than it was for the 40- by 80-foot test section strut fairings. The 80- by 120-foot test section strut fairings induce a decrease in the lift coefficient of approximately 0.017 at zero angle of attack. The presence of the 80- by 120-foot test section walls causes an increase in the lift curve slope of approximately 3% as well as a negative shift in the zero-lift angle of attack of about 0.07°. Figure 10 clearly indicates that the strut fairings are the major source of interference effects in this case. The magnitude of the corrections for the 80- by 120-foot test section is summarized in table 2.

As mentioned earlier, the strut tips used in the 80- by 120-foot test section were shorter than the ones used in the 40- by 80-foot test section, which caused the top of the fairings to be much closer to the lower surface of the wing in the 80- by 120-foot test section than they were in the 40- by 80-foot test section. An examination of the pressure distribution on the lower surface of the wing in the vicinity of the main strut attachment point provides an explanation for the increased interference effect of the struts in the 80- by 120-foot test section. Figure 11 shows the pressure coefficient on the lower surface of the wing computed by PMARC plotted versus x/c at three spanwise locations for the E-7A alone, for the E-7A in the 40- by 80-foot test section, and for the E-7A in the 80- by 120-foot test section. The main strut tips attach to the lower surface of the wing at approximately 2y/b = 0.40. As can be seen, the presence of the strut fairings in close proximity to the lower surface of the wing in the 80- by 120-foot test section causes a significant low-pressure region that effectively reduces wing lift. This causes the large strut-interference effect in the 80- by 120-foot test section.

Figure 12 shows measured lift-coefficient versus angle-of-attack data for the E-7A in the 40- by 80- and 80- by 120-foot test sections at a tunnel speed of 40 knots. The E-7A was in the conventional wing-borne flight configuration. Thrust from the ventral nozzle and the rear nozzle, which was computed by integrating exit pressure rake measurements, has been removed from the measured lift data. Part (a) of figure 12 shows the lift-coefficient data (with thrust effects removed) as measured by the wind tunnel scale system. Part (b) shows the same data after the appropriate wind tunnel wall effects (listed in table 2) have been removed. As can be seen, removing the wall effects computed using PMARC from the measured lift-coefficient data produces the same corrected lift-coefficient versus angle-of-attack curve for both tunnels. It should be noted that 40 knots represents a dynamic pressure of 5 psf, which is the practical lower limit of operation of both tunnels. At this tunnel speed, the scales systems are loaded to only a small fraction of their capacity, especially in the 80- by 120-foot test section. Thus some scatter in the force data is to be expected at this low tunnel speed.

Figures 13 and 14 present results similar to those presented in figure 12, but at tunnel speeds of 60 and 100 knots, respectively. Again, removing the wall effects computed using PMARC from the measured lift-coefficient data produces the same corrected lift-coefficient versus angle-of-attack curve for both tunnels. Note that as tunnel speed is increased, the aerodynamic loads are a larger percentage of the scales' capacity and the scatter in the data is reduced.

Conclusions

A technique for evaluating the effects of wind tunnel walls and model support hardware on the lift coefficient of a wind tunnel model has been developed using a three-dimensional, low-order panel method. The technique used the panel method PMARC to compute the flow field over a model, both with and without the presence of wind tunnel walls and model support strut fairings. The increment in model lift coefficient due to the presence of the wind tunnel walls and model support strut fairings was then evaluated and removed from corresponding experimental data to generate corrected lift-coefficient versus angle-of-attack curves. Validity of the technique was assessed by comparing the corrected lift-coefficient curves for a model that was tested in two different test sections.

The technique was applied to data from tests of the E-7A STOVL fighter model in the 40- by 80-foot and 80- by 120-foot test sections of the NFAC facility. For the 40- by 80-foot test section, the results from PMARC indicated a 10% increase in slope of the lift-coefficient versus angle-of-attack curve and a negative shift of 0.4° angle of attack at zero lift due to the presence of the wind tunnel walls. The strut fairings caused a small decrease in lift coefficient of 0.004 at zero angle of attack, which decreased at the rate of 0.000265/deg as angle of attack increased. For the 80- by 120-foot test section, the PMARC computations indicated a 3% increase in slope of the lift-coefficient versus angle-of-attack curve and a negative shift of 0.07° angle of attack at zero lift due to the presence of the wind tunnel walls. The increment in lift coefficient due to the presence of the strut fairings was larger in this case than it was for the 40- by 80-foot test section. The strut fairings caused a decrease in lift coefficient of 0.017 at zero angle of attack, which decreased at the rate of 0.000705/deg as angle of attack increased. Detailed pressure distributions computed by PMARC on the wing lower surface indicated that the closer proximity of the strut fairing to the wing in the 80- by 120-foot test section was the cause of the larger strut interference effects.

When the above effects were removed from the corresponding experimental data, the corrected lift-coefficient versus angle-of-attack curves from the two wind tunnel test sections matched very well. Thus the technique of using a three-dimensional, low-order panel method for computing wind tunnel wall and model support hardware effects on model lift coefficient in the linear lift range has been validated for the E-7A model.

Additional work is needed in a number of areas to extend this technique for computing wind tunnel wall effects. The accuracy of this technique as model size is increased relative to test section size needs to be explored. Extension of the method to predict wall effects on the lift coefficient in the nonlinear lift range and on the drag coefficient also needs to be addressed. This will require boundary-layer and separated-flow models to be added to PMARC.

References

1. Rae, W. H.; and Pope, A.: Low-Speed Wind Tunnel Testing. John Wiley & Sons, Inc., New York, 1984.
2. Ojha, S. K.; and Shevare, G. R.: Exact Solution for Wind Tunnel Interference Using the Panel Method. Computers and Fluids, vol. 13, no. 1, 1985, pp. 1–14.
3. Bowcutt, K. G.: The Use of Panel Methods for the Development of Low-Subsonic Wall Interference and Blockage Corrections. AIAA Paper 85-0159, Jan. 1985.
4. Lee, K. D.: Numerical Simulation of the Wind Tunnel Environment by a Panel Method. AIAA Paper 80-0419, Mar. 1980.
5. Holt, D. R.; and Hunt, B.: The Use of Panel Methods for the Evaluation of Subsonic Wall Interference, AGARD CP-335, May 1982, pp. 2–1 to 2–16.
6. Ashby, D. L.; Dudley, M. R.; and Iguchi, S. K.: Development and Validation of an Advanced Low-Order Panel Method. NASA TM-101024, Oct. 1988.
7. Ashby, D. L.; Dudley, M. R.; Iguchi, S. K.; Browne, L.; and Katz, J.: Potential Flow Theory and Operation Guide for the Panel Code PMARC. NASA TM-102851, Jan. 1988.
8. Poppen, W. A.; Smith, B. E.; and Lye, J. D.: Propulsion-Induced Aerodynamics of an Ejector-Configured STOVL Fighter Aircraft. AIAA Paper 91-0765, Jan. 1991.
9. Foley, W.H.; Sheridan, A.E.; and Smith, C.W.: Study of Aerodynamic Technology for Single-Cruise-Engine V/STOL Fighter Attack Aircraft: Phase I Final Report. NASA CR-166268, Feb. 1982.

Table 1. Reference dimensions of the E-7A model

AR	1.665
b	32.4 ft
$\bar{c}$	23.56 ft
S	630.6 ft^2
Λ_{LE}	60°
Λ_{TE}	–10°
λ	0.115
Airfoil	NACA 63004
Moment reference point (in model coordinates)	x = 324.37 in. y = 0.0 in. z = –6.0 in.

Table 2. Wind tunnel wall and mounting hardware effects on the lift coefficient of the E-7A computed using PMARC

Strut fairing effects	
40- by 80-foot test section	80- by 120-foot test section
$\Delta CL_{\alpha_{\text{strut fairings}}} = -0.000265/\text{deg}$	$\Delta CL_{\alpha_{\text{strut fairings}}} = -0.000705/\text{deg}$
$(\Delta CL_{\text{strut fairings}})_{\alpha=0} = -0.0039$	$(\Delta CL_{\text{strut fairings}})_{\alpha=0} = -0.0168$

Wind tunnel wall effects	
40- by 80-foot test section	80- by 120-foot test section
$\Delta\alpha = -0.381^{o}$	$\Delta\alpha = -0.073^{o}$
$\frac{CL_{\alpha_{\text{E-7A/strut fairings}}}}{CL_{\alpha_{\text{E-7A/strut fairings/tunnel walls}}}} = 0.907$	$\frac{CL_{\alpha_{\text{E-7A/strut fairings}}}}{CL_{\alpha_{\text{E-7A/strut fairings/tunnel walls}}}} = 0.971$

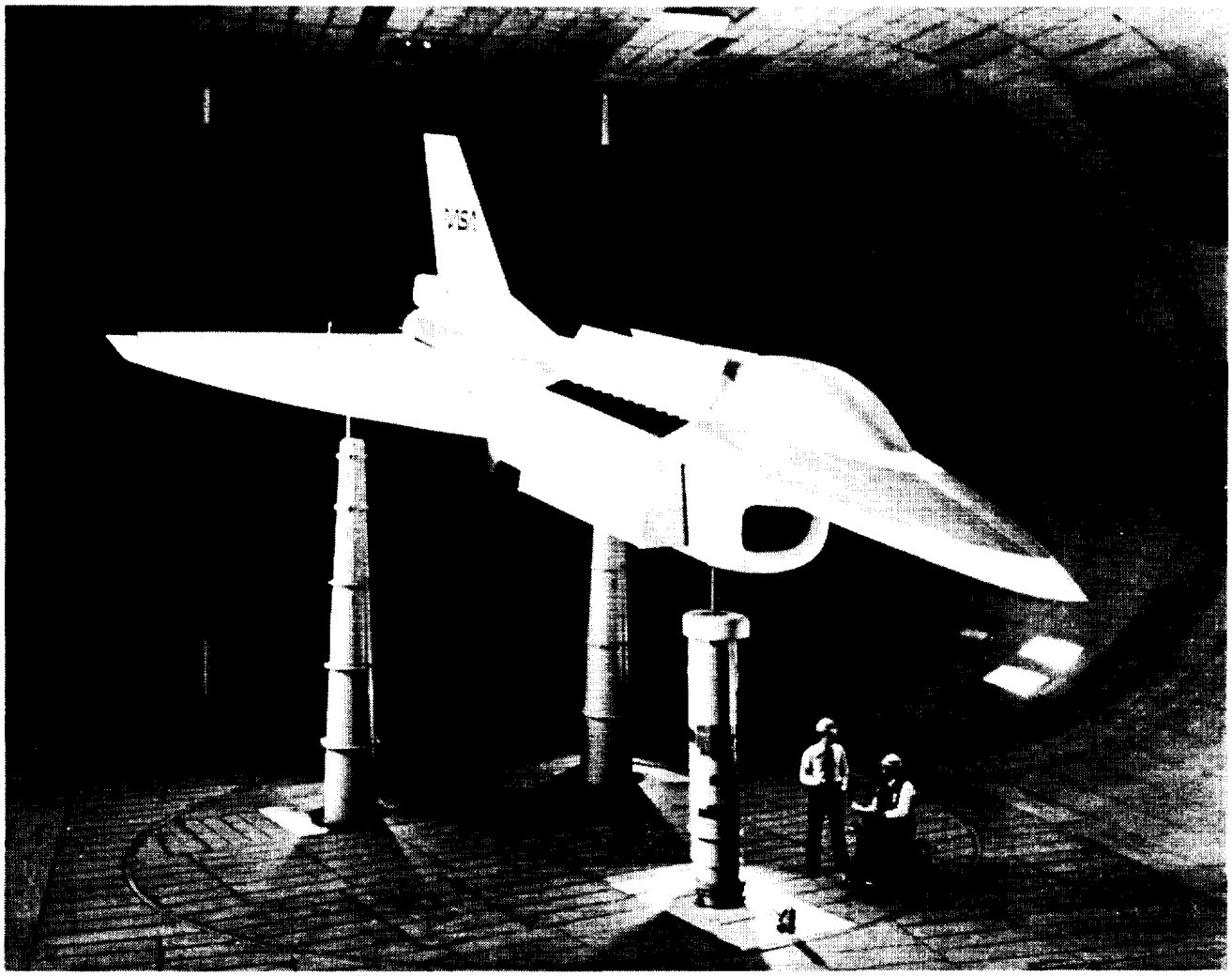

Figure 1. The E-7A model (in transition flight configuration) in the 40- by 80-foot test section of the NFAC facility.

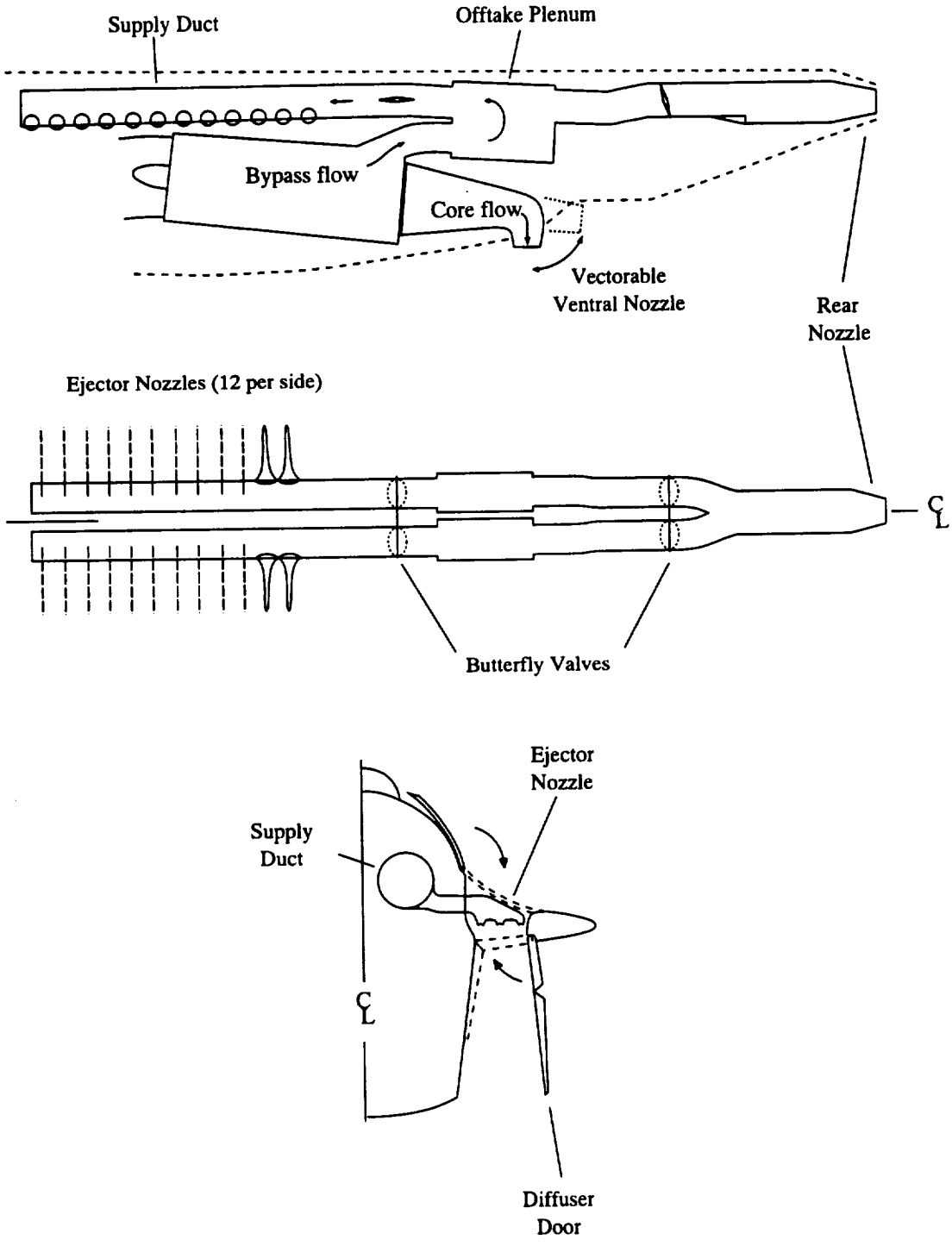

Figure 2. Schematic of the E-7A model propulsion system.

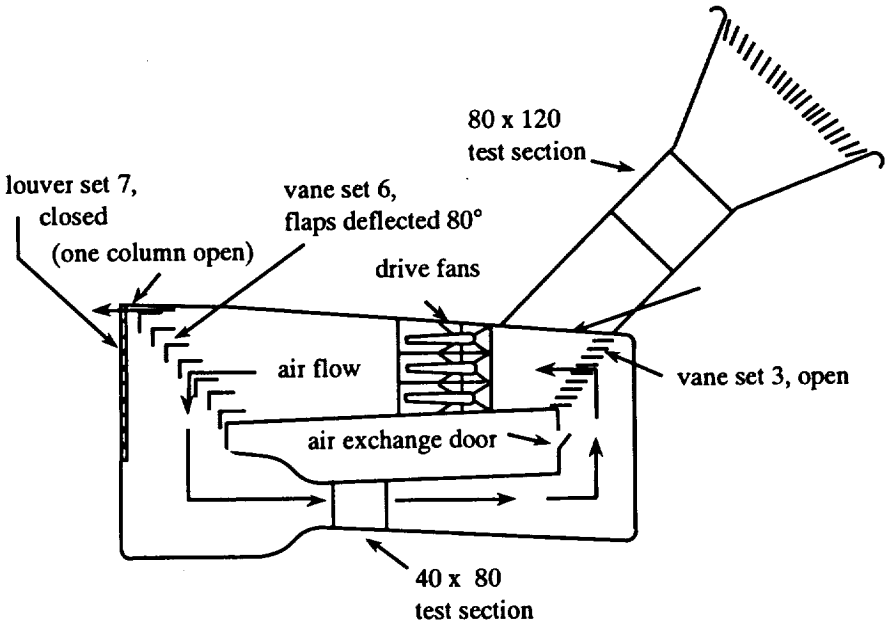

Figure 3. Schematic of the National Full-Scale Aerodynamics Complex (NFAC) in the 40- by 80-foot mode.

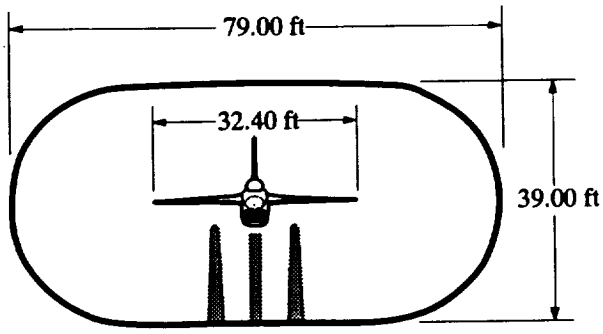

Figure 4. E-7A model in the 40- by 80-foot test section.

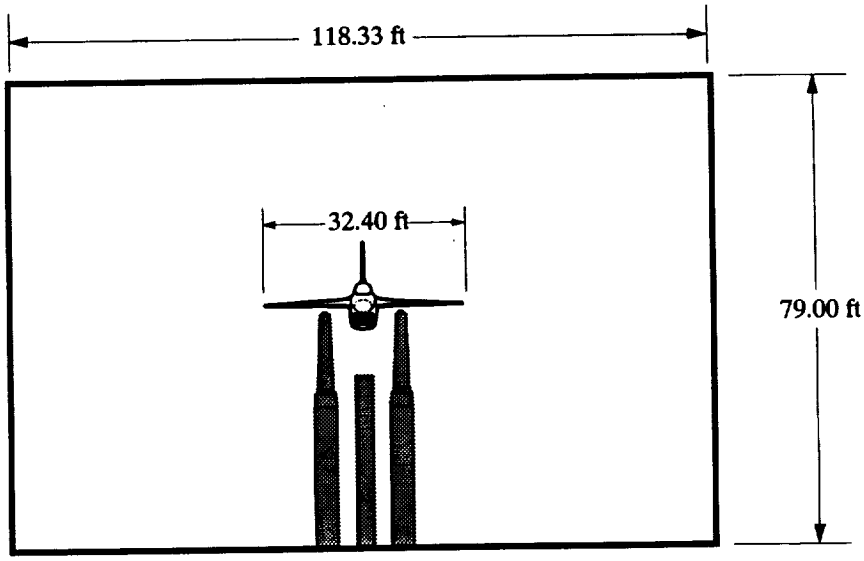

Figure 5. E-7A model in the 80- by 120-foot test section.

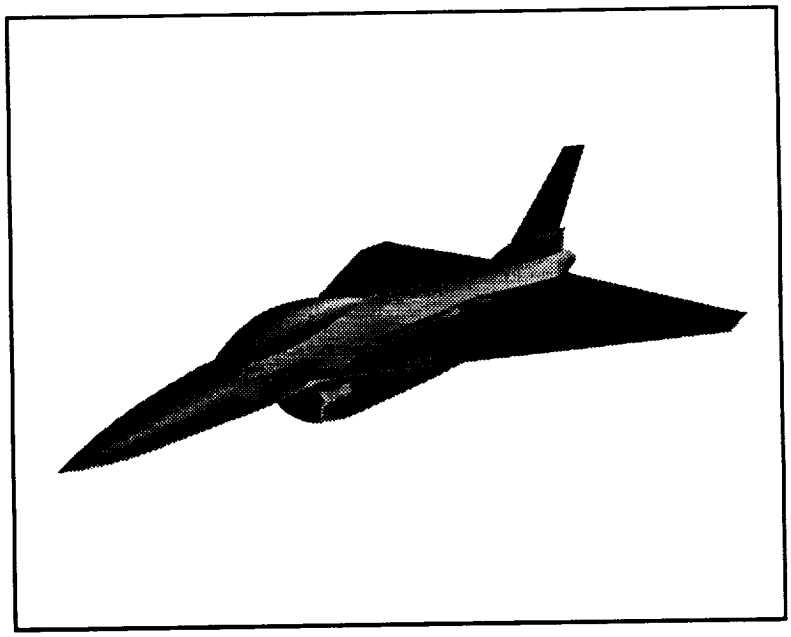

Figure 6. PMARC representation of the E-7A model in conventional wing-borne flight configuration.

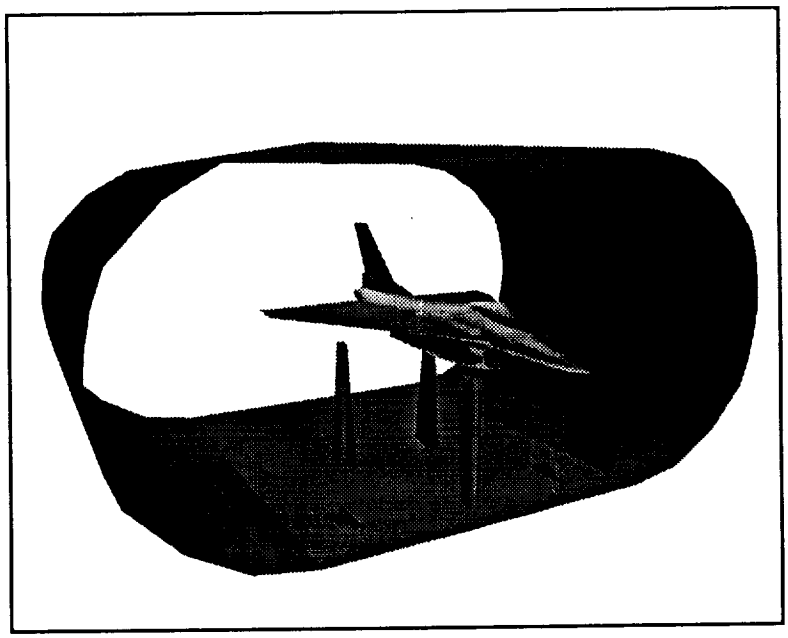

Figure 7. PMARC representation of the E-7A model in the 40- by 80-foot test section of the NFAC facility.

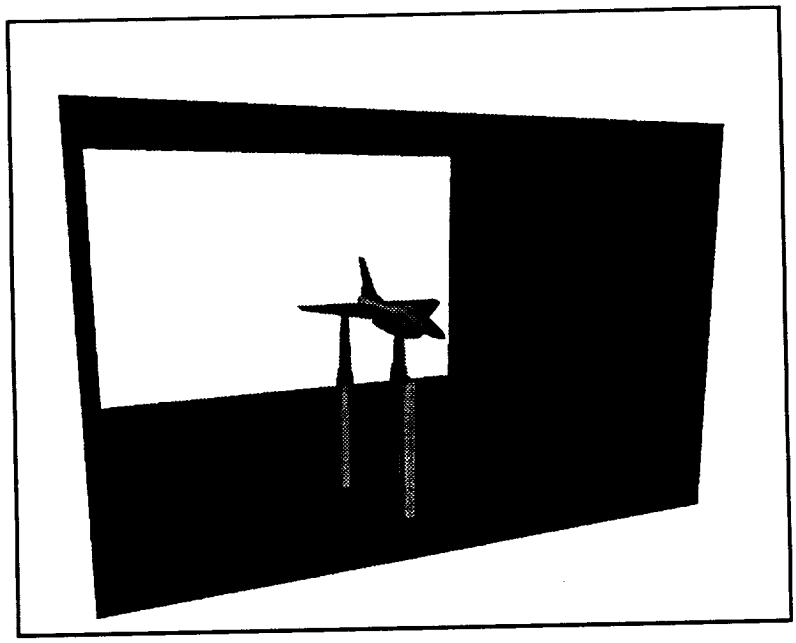

Figure 8. PMARC representation of the E-7A model in the 80- by 120-foot test section of the NFAC facility.

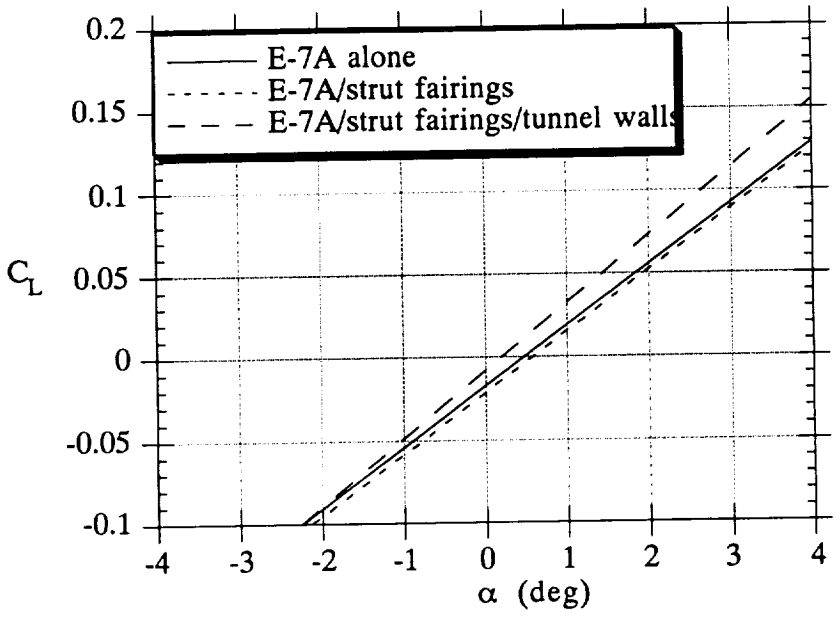

Figure 9. Comparison of C_L for the E-7A model as computed by PMARC for the E-7A alone, the E-7A with strut fairings, and the E-7A with strut fairings and 40- by- 80-foot tunnel walls.

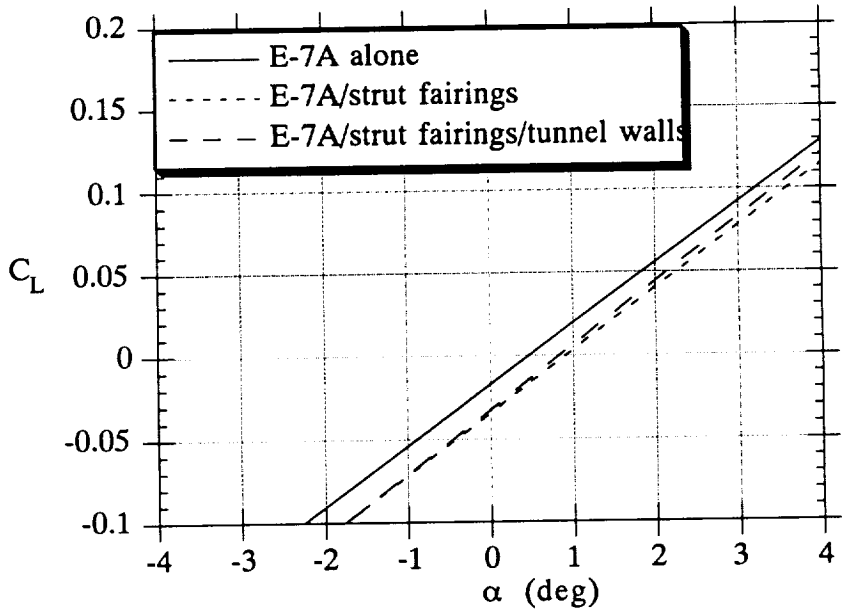

Figure 10. Comparison of C_L for the E-7A model as computed by PMARC for the E-7A alone, the E-7A with strut fairings, and the E-7A with strut fairings and 80- by- 120-foot tunnel walls.

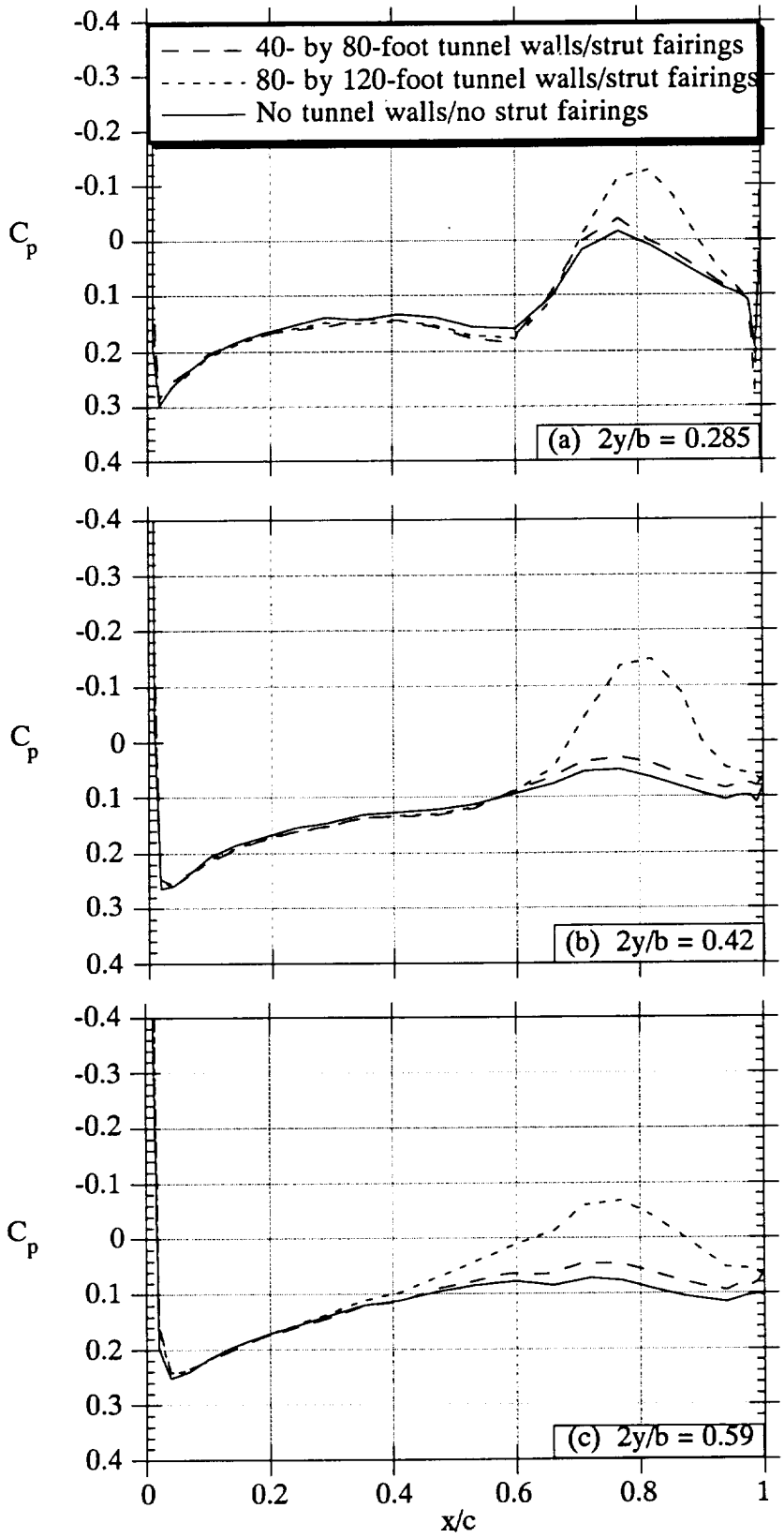

Figure 11. Comparison of C_P computed by PMARC on wing lower surface near the strut mount for the E-7A alone, the E-7A in the 40- by 80-foot test section, and the E-7A in the 80- by 120-foot test section.

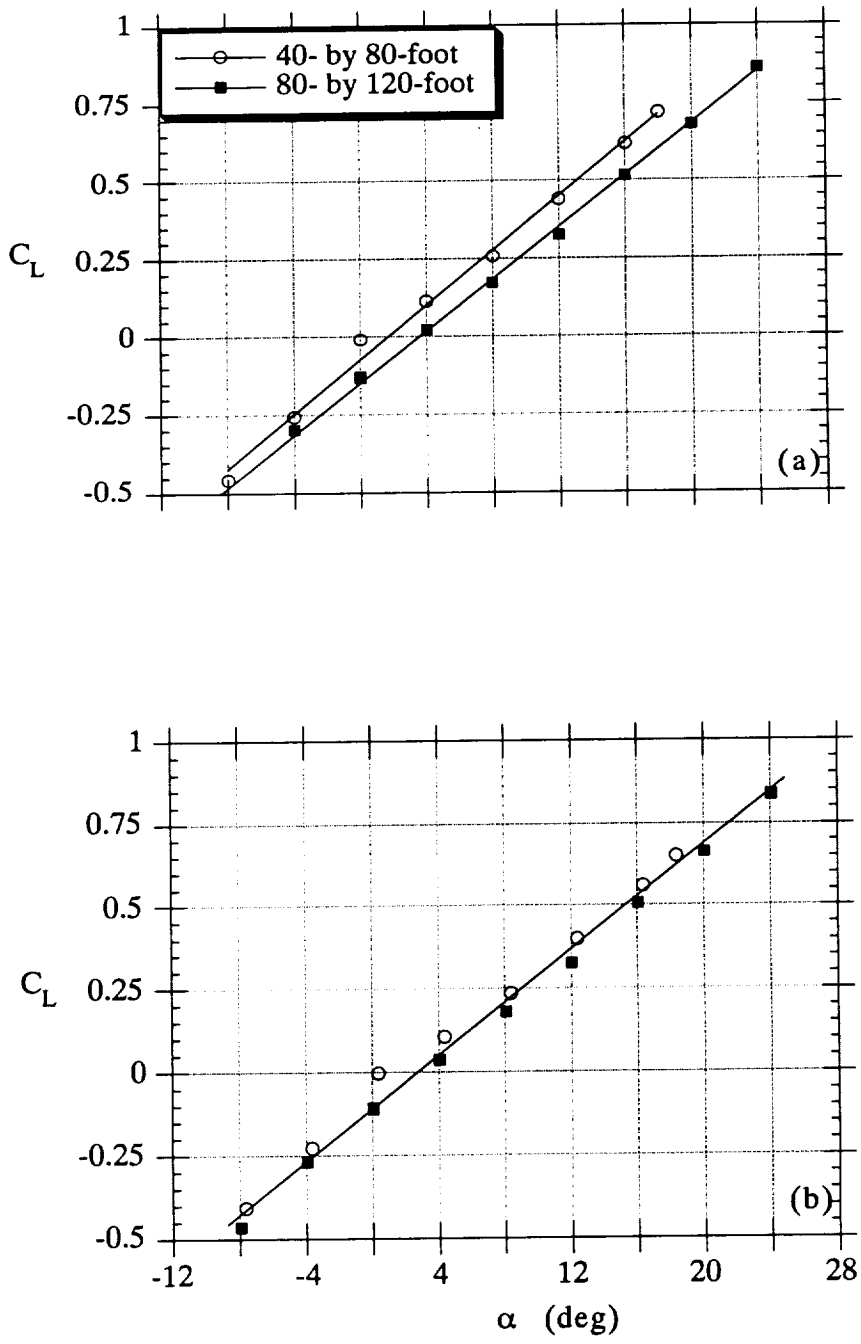

Figure 12. Comparison of (a) uncorrected and (b) corrected lift coefficient data for the E-7A in the 40- by 80-foot and 80- by 120-foot test sections. (Conventional wing-borne flight configuration, thrust removed, V∞ = 40 knots.)

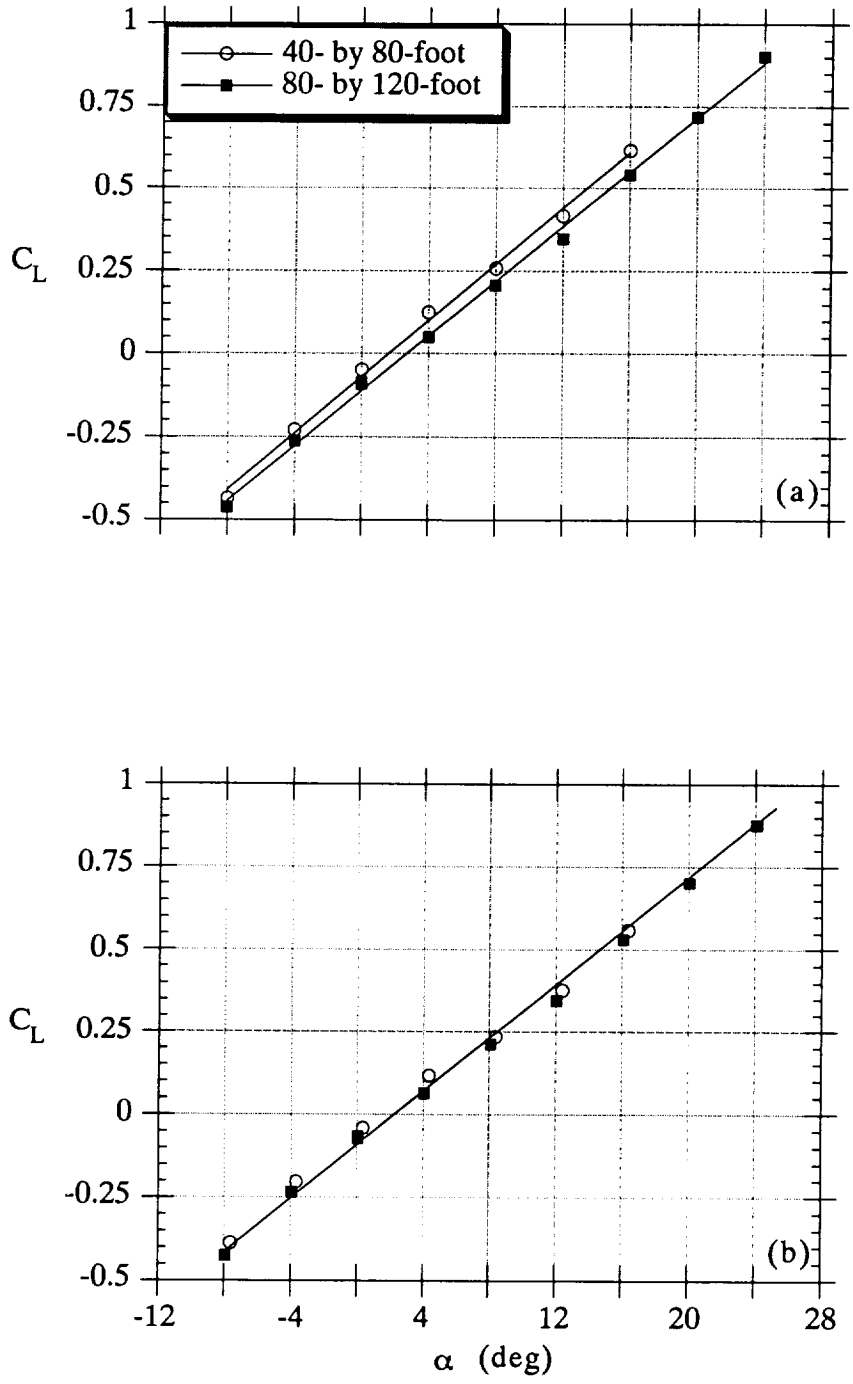

Figure 13. Comparison of (a) uncorrected and (b) corrected lift coefficient data for the E-7A in the 40- by 80-foot and 80- by 120-foot test sections. (Conventional wing-borne flight configuration, thrust removed, V_∞ = 60 knots.)

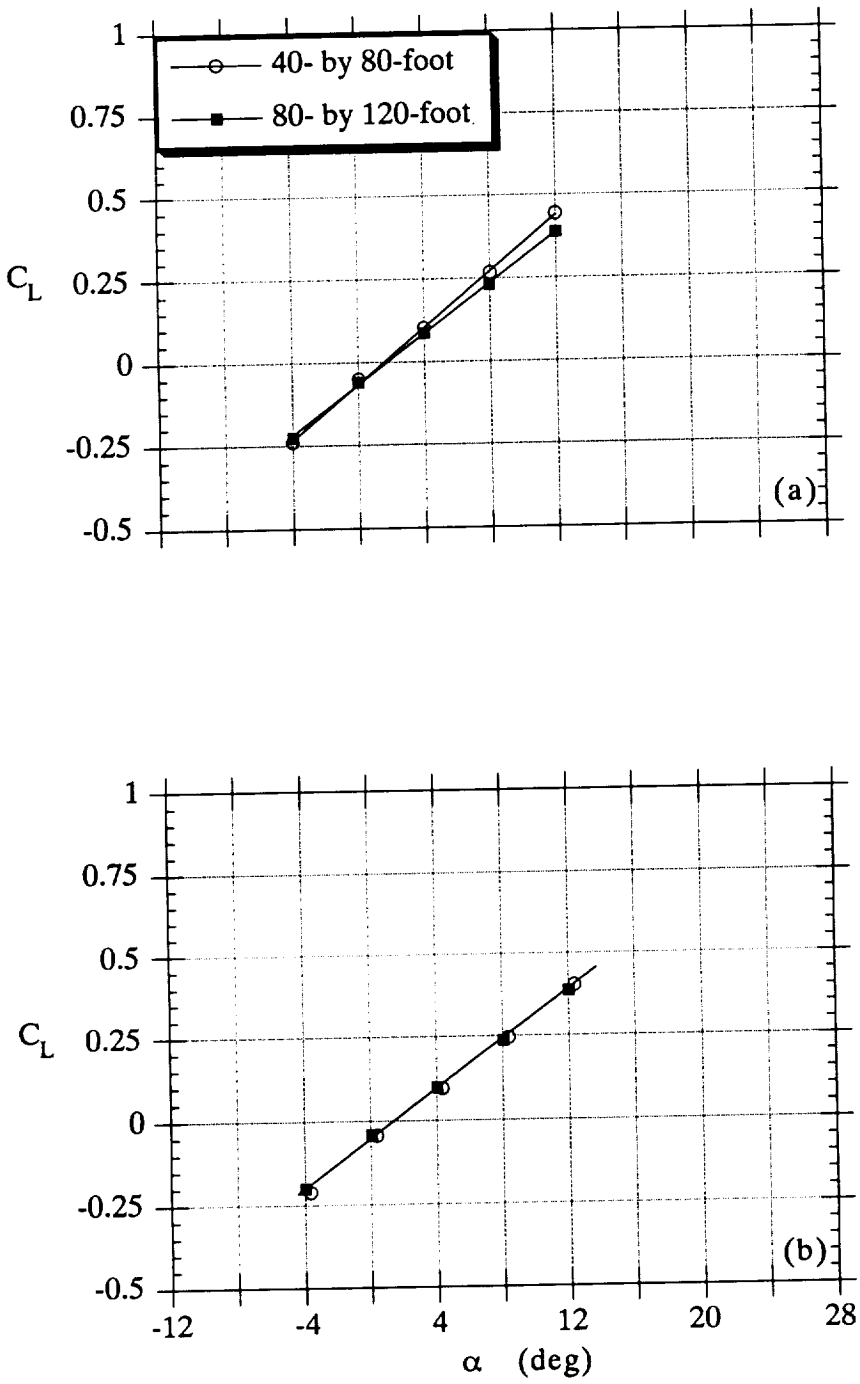

Figure 14. Comparison of (a) uncorrected and (b) corrected lift coefficient data for the E-7A in the 40- by 80-foot and 80- by 120-foot test sections. (Conventional wing-borne flight configuration, thrust removed, V_∞ = 100 knots.)

REPORT DOCUMENTATION PAGE

Form Approved
OMB No. 0704-0188

1. AGENCY USE ONLY *(Leave blank)*	2. REPORT DATE	3. REPORT TYPE AND DATES COVERED
	February 1994	Technical Memorandum

4. TITLE AND SUBTITLE
Computation of Wind Tunnel Wall Effects for Complex Models Using a Low-Order Panel Method

5. FUNDING NUMBERS
505-59-53

6. AUTHOR(S)
Dale L. Ashby and Scott H. Harris

7. PERFORMING ORGANIZATION NAME(S) AND ADDRESS(ES)
Ames Research Center
Moffett Field, CA 94035-1000

8. PERFORMING ORGANIZATION REPORT NUMBER
A-93077

9. SPONSORING/MONITORING AGENCY NAME(S) AND ADDRESS(ES)
National Aeronautics and Space Administration
Washington, DC 20546-0001

10. SPONSORING/MONITORING AGENCY REPORT NUMBER
NASA TM-104019

11. SUPPLEMENTARY NOTES
Point of Contact: Dale L. Ashby, Ames Research Center, MS 247-2, Moffett Field, CA 94035-1000
(415) 604-5047

12a. DISTRIBUTION/AVAILABILITY STATEMENT
Unclassified — Unlimited
Subject Category 02

12b. DISTRIBUTION CODE

13. ABSTRACT *(Maximum 200 words)*

A technique for determining wind tunnel wall effects for complex models using the low-order, three-dimensional panel method PMARC (Panel Method Ames Research Center) has been developed. Initial validation of the technique was performed using lift-coefficient data in the linear lift range from tests of a large-scale STOVL fighter model in the National Full-Scale Aerodynamics Complex (NFAC) facility. The data from these tests served as an ideal database for validating the technique because the same model was tested in two wind tunnel test sections with widely different dimensions. The lift-coefficient data obtained for the same model configuration in the two test sections were different, indicating a significant influence of the presence of the tunnel walls and mounting hardware on the lift coefficient in at least one of the two test sections. The wind tunnel wall effects were computed using PMARC and then subtracted from the measured data to yield corrected lift-coefficient versus angle-of-attack curves. The corrected lift-coefficient curves from the two wind tunnel test sections matched very well. Detailed pressure distributions computed by PMARC on the wing lower surface helped identify the source of large strut interference effects in one of the wind tunnel test sections. Extension of the technique to analysis of wind tunnel wall effects on the lift coefficient in the nonlinear lift range and on drag coefficient will require the addition of boundary-layer and separated-flow models to PMARC.

14. SUBJECT TERMS
Panel method, Wall correction, Wind tunnel testing

15. NUMBER OF PAGES
20

16. PRICE CODE
A03

17. SECURITY CLASSIFICATION OF REPORT	18. SECURITY CLASSIFICATION OF THIS PAGE	19. SECURITY CLASSIFICATION OF ABSTRACT	20. LIMITATION OF ABSTRACT
Unclassified	Unclassified		